THESIS FOR THE DEGREE OF LICENTIATE OF ENGINEERING

Water-assisted mixing and compression moulding of ethylene-acrylic acid copolymer reinforced with nano-cellulose

ABHIJIT VENKATESH

Department of Industrial and Materials Science
CHALMERS UNIVERSITY OF TECHNOLOGY
Gothenburg, Sweden 2018

Water-assisted mixing and compression moulding of ethylene-acrylic acid copolymer reinforced with nano-cellulose

ABHIJIT VENKATESH

Technical report Nr: IMS-2018-15

Department of Industrial and Materials Science
Chalmers University of Technology
SE-412 96 Gothenburg
Sweden
Telephone + 46 (0)31-772 1000

Cover:
Composites containing 20 vol.% of nanocellulose compared with composites containing pulp of similar concentration.

Printed by Chalmers Reproservice
Gothenburg, Sweden 2018

Water-assisted mixing and compression moulding of ethylene-acrylic acid copolymer reinforced with nano-cellulose

ABHIJIT VENKATESH

Department of Industrial and Materials Science
Chalmers University of Technology

ABSTRACT

The concerns regarding aspects of global warming, depleting oil resources, accumulation of plastics in landfills has served as motivation to move towards utilizing sustainable and renewable resources to fulfil our needs. In the present work, the reinforcing capabilities of cellulose nanofibrils (CNF) and modified/unmodified cellulose nanocrystals (CNC) based composites prepared through water-assisted mixing, drying and compression moulding was explored. At the water-assisted mixing, compositions consisting of an aqueous dispersion of a poly(ethylene-co- acrylic acid) copolymer, nanocellulose suspension and excess water of about 96 %, were used to prepare the composites. The final composites had a dry loading content of 10 to 70 vol.% CNF or 0.1 – 10 wt.% CNC.

The CNF based composites showed an increase in strength and stiffness with increasing cellulose nanofibril content. At the highest loading content of 70 vol.% the composites exhibited an improved strength and stiffness by a factor of 3.5 and 21, respectively while still maintaining an elongation of 5 %. The composites with 20 vol.% cellulose content confirmed a well dispersed reinforcement in the matrix through computed tomography. The composites had a stiffening threshold around 30 vol.% CNF content which coincided with the CNF concentration at which the effective stiffness of the composite was maximum. Furthermore, the strength and strain at break of CNF composites were higher than pulp based composites but the same could not be said for the stiffness. The CNC based composites on the other hand showed a strong influence of the CNC on yield behaviour and ductility of the composites, especially at higher CNC contents (10 wt.%). Dynamic mechanical analysis revealed indications of strong interactions between the grafted components and the matrix or between the grafted components themselves which was confirmed by the mechanical test data. However, the improved thermal stability of the modified CNC (almost 100 °C improvement) was not observed when they were introduced into the composites owing to alkalinity of the matrix that resulted in degrafting.

Keywords: Nanocellulose, cellulose nanocrystals, cellulose nanofibrils, amphiphilic co-polymer, azetidinium, rheology, thermal stability, water-assisted mixing.

LIST OF PUBLICATIONS

The thesis is based on results contained in the following papers, referred to by Roman numerals in the text.

I Cellulose nanofibril-reinforced composites using aqueous dispersed ethylene-acrylic acid copolymer
Venkatesh A, Thunberg J, Moberg T, Klingberg M, Hammar L, Peterson A, Müller C, Boldizar A
(2018) *Cellulose*, 25(8) p. 4577-4589
doi: 10.1007/s10570-018-1875-3

II Composites with surface-grafted cellulose nanocrystals (CNC)
L. Forsgren, K. Sahlin, A. Venkatesh, J. Thunberg, R. Kádár, A. Boldizar, G. Westman & M. Rigdahl
Manuscript, submitted for publication.

Table of Contents

1
INTRODUCTION

1.1 Background

The plastic revolution began when celluloid was invented in late 1800's which showcased that humanity was no longer constrained by the limits set by nature. Even though the intention was to replace ivory as raw material, it wasn't too long before these thermoplastics entered the consumer market [1]. These non-degradable entities have contaminated the environment and at present 79 % of the 8300 million metric tons of plastic produced from 1950 - 2015 have accumulated in the environment [2]. These concerning statistics is supported by the awareness and increasing demands from the society to move towards a more sustainable future. This can be done by opting to replace or reduce the use of fossil based non-degradable plastics by bio-based, biodegradable and renewable replacements. A candidate in this case would be cellulosic materials which are biodegradable, renewable, abundant and inexpensive.

The use of natural cellulosic materials as structural material has been around for centuries and they still compose a large part of industries like paper, forest products, textiles, *etc*. The Swedish forest industry, which is a model for being the most sustainable forest industries, has always used cellulose as raw materials in various application ranging from printing media, packaging to construction [3]. The main source of cellulose are lignocellulosic plants and trees, with a global annual synthesis of 100 billion tons, and hence abundantly available in nature [4]. It is inexpensive and known for its ability as an efficient structural reinforcement in plants and can also be obtained from tunicates, algae and bacteria.

With the current dominance of electronic media, the need for printed media has been declining and this permits the forest industry to invest more in the usage of the wood pulp based materials in other applications leading to material innovation. Furthermore, the strict regulations from EU are pushing industries such as the automotive sector to opt for more sustainable materials/solutions and this has worked in favour of wood based materials which can be used as reinforcement in composites due to their promising mechanical properties [5]. When compared to the glass fibre reinforced composites (GFRC), the cellulose fibre reinforcement have low density, exciting mechanical properties due to their hierarchical structure, relatively low cost, low abrasive nature, non-hazardous handling, possibility for chemical modification (due to the large density of hydroxyl groups), better end-of-life phase and possibility to be melt processed [6]. The "greener footprint" due to their lower

environmental impact, lighter weight and better end-of-life phase could also serve as reasons for using these cellulose fibers as reinforcements in plastics/composites instead of non-renewable glass fibers [6].

However, the favourable properties of cellulose also have drawbacks, especially in terms of being a natural material which would result in various size of fibres/fibrils compared to glass fibres. Furthermore, the fibre-matrix adhesion can be inefficient while using the hydrophilic cellulose as reinforcements in a hydrophobic thermoplastic matrix [7]. The non-uniform reinforcement dispersion, agglomeration, moisture uptake and the rather well known low thermal stability of cellulose are also limiting factors in their usage as efficient reinforcements in thermoplastic polymers. The low thermal stability causes discolouration and limits the processing temperature and types of matrices that can be used with cellulose fibrils [8].

1.2 Aim and Outline of the Thesis

The interest in nanocellulose as a potential reinforcement is generally motivated by the expected applications in society. This makes it important to understand the effect of process structuring and its parameters on the functional properties, in this case nano-cellulose reinforced composites, with a view on large scale manufacturing processes. This is the aim of the work and special emphasis has been given to wet based mixing techniques in order to explore their viability.

In the current study, the aim of the work can be based on the reinforcements used and the common objective of exploring the effect of water assisted mixing on the mechanical properties of composites reinforced by cellulose nanofibrils (CNF) and cellulose nanocrystals (CNC):

Paper I explored the possibility to achieve high CNF loading contents in the composites while still being able to maintain best possible dispersion and mechanical properties.

Paper II studies was based on the CNC composites, the effect of CNC modification on thermal stability and mechanical properties.

2

CELLULOSE REINFORCED THERMOPLASTICS

2.1 Cellulose and its Morphology

Cellulose is nature's own reinforcing structure found mainly in cell wall of all plants as well as in some tunicates, algae and bacteria. It is a composed of linearly chained glucose monomers connected together by β 1-4 glycosidic bond, see figure 1. The cellulose chain has a linear configuration due to the intra-chain hydrogen bonding between the OH- groups and oxygen in the adjoining chains [9]. The stability, insolubility in water and high axial strength of cellulose is due to these strong intra and inter molecular hydrogen bonding of the chains. They are fibrous, semi-crystalline as observed in the fibrils which contain highly ordered and disordered regions and embedded in an amorphous matrix consisting of lignin, hemicellulose, pectin, waxes and are normally the components responsible for the structural integrity in a tree [10]. The fibres that reinforce the tree are part of a hierarchical structure which in the macroscale consist of a fibres connected to each other by a layer of lignin and hemicellulose to form a fibre bundle, see figure 2. Each fibre in these bundles are made up of cellulose microfibrils, which constitutes the microscale, and these microfibrils are made of cellulose nanofibrils or individual fibrils, which constitute the nanoscale.

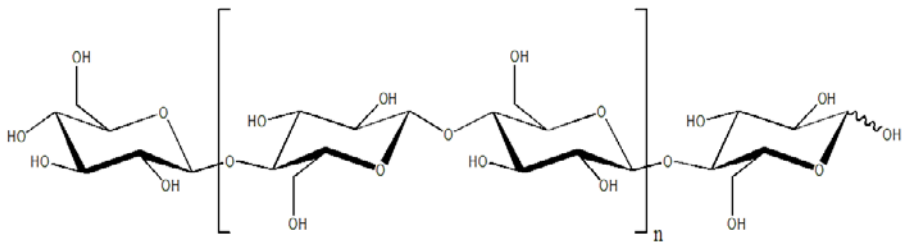

Figure 1: Molecular structure of cellulose.

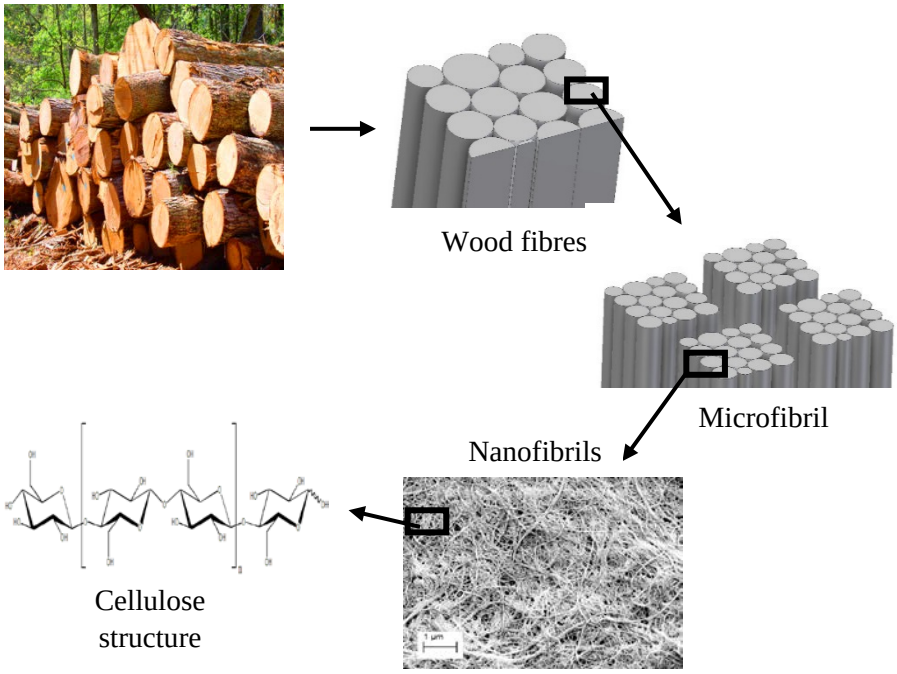

Figure 2: Hierarchical structure of wood from tree to cellulose.

2.2 Cellulose Nanofibrils

The hierarchical structure of cellulose in which at least one of the dimension are in nanometre scale are considered as nanocellulose. Cellulose nanofibrils (CNF) contains both the ordered region (crystalline) and the disordered region (non-crystalline) with lengths up to a few µm [9]. Depending whether it is a single fibril or a bundle of fibrils, their diameters will vary from 3 – 5 nm to 15-20 nm, respectively [11]. The recent developments in pulp processing has reduced the energy demands to produce CNF due to which they are available commercially [12]. They are produced by delamination of fibre either by intense mechanical treatment (homogenization with several passes) or a combination of chemical or enzymatical pre-treatment (introduction of charged groups) followed by homogenization [13]. The resulting suspension forms an aqueous gel at low concentration because of the increased surface area due to delamination and fibrillation.

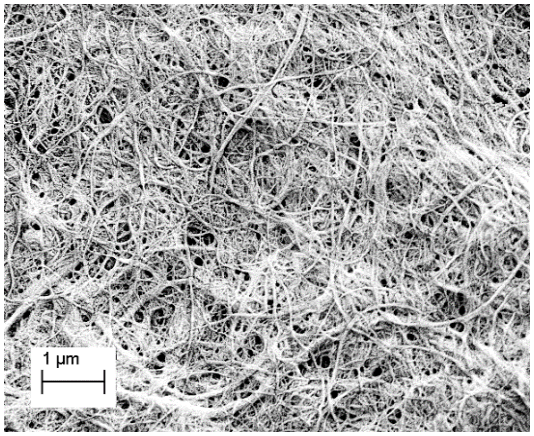

Figure 3: Scanning electron micrograph of dried nanocellulose fibrils.

2.3 Cellulose Nanocrystals

Cellulose nanocrystals (CNC) are stiff, highly crystalline and rod like shaped cellulose derivatives which are obtained when the amorphous part of the cellulose nanofibrils are removed through acid-catalysed hydrolysis [14]. Their dimensions vary from 5 - 50 nm in diameter to 100 - 500 nm in length based on their source and extraction method [4]. CNC in aqueous suspensions can exhibit a liquid crystalline behaviour depending on the concentration, CNC dimensions, ionic strength and type of counter-ion [11]. CNC suspensions also exhibit gel-like behaviour but with viscosity lower than that of the CNF due to the difference in aspect ratio of the nanoparticles. There are mainly two acids used to produce CNC's which are sulphuric acid and hydrochloric acids. The former creates CNC functionalized with sulphate half ester groups which provides good colloidal stability but compromises the thermal stability. On the other hand, hydrochloric acid method produces CNC's with good thermal stability but poor colloidal stability due to the absence of charged species [15].

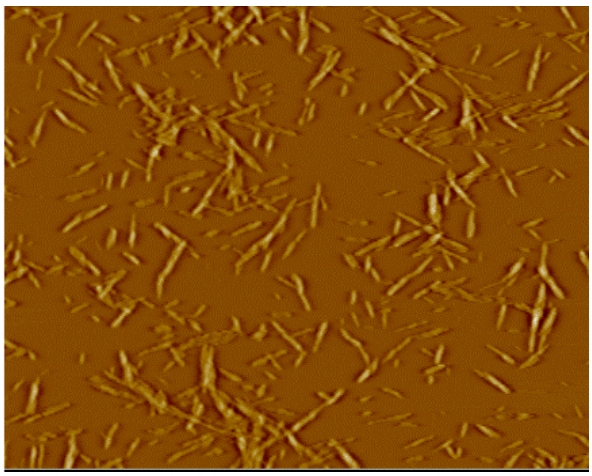

Figure 4: Atomic force micrograph of dried nanocrystals.

2.4 Surface Modification of Cellulose Nanocrystals

CNCs have an abundance of OH- groups on their surface which make it accessible to chemical surface modification. Modifications by addition of functional group can reduce hydrophilicity of CNC and also moderate the amount of accessible sulphate groups. These sulphate groups occur during acid hydrolysis and are responsible for the poor thermal stability of CNC. Furthermore, the grafted chemical groups can help improve the compatibility between the CNC's and the matrix material to improve properties. In this work, azetidinium salts have been used to graft functional groups onto sulphate groups of CNC [16].

2.5 Cellulose as Reinforcement in Thermoplastics

Wood particles as reinforcement/filler, in the form of saw dust, wood chips or natural fibre fractions, in thermoplastics has been studied since decades [8, 17–19]. Since the 1990s, the automotive industry has shown strong interest to use cellulose based materials as reinforcement compared to GFRC. The lower environmental impact, the need for higher fibre loading content to reach equivalent GFRC performance (reduces the amount of fossil based matrix material used) and recyclability have made them a realistic alternative to GRPC in these applications. Furthermore, the recent developments in pulp processing has further strengthened their role as alternative reinforcements, owing to commercial availability of nanocellulose, and these high strength and aspect ratio based materials are regarded as better reinforcing agents in composites compared to cellulose fibre [20, 21, 7].

The nanocellulose usually have higher aspect ratio, strength and stiffness compared to cellulose fibres. But their hydrophilic nature still remains and this this drastically affects their ability to reinforce a hydrophobic polymer. This leads to problems regarding moisture absorption, agglomeration, poor fibre-matrix adhesion, poor wetting and inefficient stress transfer [22]. The need for efficient stress transfer is vital in a composite to improve the mechanical properties which means that the surface area of contact between the matrix and the reinforcing material is vital. Even though nanocellulose have a high specific surface area they also have a higher tendency to agglomerate and these agglomerates behave like stress concentration which means that the true reinforcing capabilities of the nanocellulose are hardly accurately realized. In addition, the selection of matrices when cellulose is a reinforcement is limited due to its degradation at relatively low temperature. In order to obtain a well dispersed composite there has been emphasis on processing techniques, compatibilzation and surface modification which will be discussed in the upcoming section.

2.6 Poly(ethylene acrylic acid)

Poly(ethylene acrylic acid) (EAA) is an amphiphilic, semi-crystalline, random co-polymer which finds its applications in coatings, packaging, *etc* [23]. It consists of an ethylene backbone with random carboxyl pendants, see figure 5. The amount of acrylic acid (AA) in the polymer influences the physical properties of the polymer. The hydrophilicity increases with AA content, the crystallinity and melting point reduces with increasing AA. Thicker crystalline lamellas are obtained with lower AA content as there is less hydrogen bonding interfering with the crystallization behaviour. The presence of low temperature melting peak, below the primary melting peak, is also observed in the DSC measurements attributable to the melting of thin secondary PE crystallites that form during cold crystallization [24].

EAA has shown to be compatible with cellulose and its lower melting temperature of 80 to 110 °C reduces the risk of thermal degradation of the additives which makes it an interesting matrix for cellulose based composites [22]. Furthermore, the combination of properties, like flexibility, chemical resistance, barrier properties of the ethylene molecules with the polarity, toughness and hot tack strength of AA adds to the benefit of selecting EAA as a matrix [25].

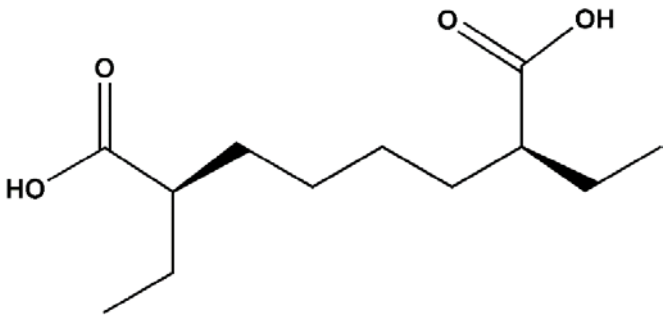

Figure 5: Molecular structure of EAA with acrylic acid sections.

3

PROCESSING OF NANOCELLULOSE REINFORCED COMPOSITES

3.1 Fundamental Problems

The melt-processing aspects of cellulose nanocomposites is not well understood. This knowledge deficit is likely a major obstacle for large scale application that would decide the final properties, like dispersion, alignment and agglomeration, which defines the mechanical strength of the material. Hence, substantial effort needs to be devoted to compatibility and adhesion issues, avoiding agglomeration and non-uniform dispersion of the reinforcing phase, all leading to poor mechanical properties. Furthermore, the consequences due to the thermal degradation of cellulose needs to be better understood. Hence, the matrices commonly used are limited to relative low melting temperature based polymers [26, 27].

In order to address the above problems while still being able to obtain a well dispersed nanocomposite, there has been works to hydrophobize the cellulose surface through grafting, physical adsorption of surfactants and amphiphilic copolymers [28–30]. These methods have been effective in improving compatibility and dispersion but utilize non-polar solvents and multiple reaction steps which limit their industrial relevance. On the other hand, solvent casting of nanocellulose is known to yield a well dispersed composite with excellent mechanical properties [31, 32]. However, the results are much better when an insoluble aqueous dispersion is used than a water-soluble polymer [28, 33, 34].

Cellulose nanocomposites can be manufactured by a number of approaches like solution casting, melt processing techniques, resin impregnation of nanofiber preforms and many more. However in this thesis, the focus is on solution casting and melt processing techniques compression moulding.

3.2 Wet Mixing Method

Liquid assisted mixing technique has been seen as a promising way to process cellulose based nanocomposites and this method is commonly used in nano-clay based composites [35–39]. The matrices usually used when adopting liquid assisted mixing are polar matrices like PA, PVA, TPS etc. while apolar matrices needed the presence of compatibilizers to be effective [39]. The liquid-assisted technique can be considered as a useful way to disperse nanocellulose in the presence of high water content. It can be coupled with the presence of high shear forces to further improve the dispersion. The technique reduces the need for surface modification, degradation of the surface fillers can be reduced, health concerns are minimal due to the slurry form of the nanomaterial and it is suggested that the ‘blow up’ phenomenon due to evaporation of pressurized liquid especially water could help dispersion.

This method has also exhibited the possibility for having higher cellulose loading (> 50 wt %) while maintaining good mechanical properties for cellulose fibers [40].

3.3 Compression Moulding

Compression moulding is a conventional melt processing technique which is commonly used for cellulose based composites. When compared to injection moulding the sample here is exposed to both temperature and pressure but less fibre orientation is observed [41]. The mould design is usually simple and efficient for mostly low production volumes which reduces costs [42]. The raw material is loaded in the form of sheets (films), pellets or powder but usually film or ply stacking is recommended as it reduces the chance of a grainy structure e.g. due to domains with less degree of mixing or due to the joining of melts in the composite [43]. Furthermore, the application of pressure during and after the softening temperature helps in reducing shrinkage effects.

4
EXPERIMENTAL

4.1 Materials

4.1.1 Cellulose Nanofibrils

In paper I, the CNF used, type Exilva was obtained from Borregaard A/S, Norway. The raw material for these CNFs, which came in the form of a 10 wt.% paste in water, were from Norwegian spruce sulphite pulp. The weight fraction of the different components are as shown in Table 1.

4.1.2 Reference Pulp Fibres

As a reference in paper I, the cellulose fibre pulp used was provided by Nordic Paper Seffle AB, Sweden. The pulp was a highly beaten never dried bleached softwood mixture of 80 % spruce sulphite and 20 % spruce sulphate pulp. The weight fraction of the different components are shown in Table 1.

Table 1: Cellulose content obtained through Monosaccharide Carbohydrate Analysis

Cellulose Type	Klason lignin (wt.%)	Hemicellulose (wt.%)	Cellulose (wt.%)
CNF	3.2	2.8	94
Pulp	1.9	17	80

4.1.3 CNC and Modifications

In paper II, the untreated aqueous CNC dispersions were obtained through sulphuric acid hydrolysis of microcrystalline cellulose using a method described by Sahlin et al., 2018, which is a modification of the procedure outlined previously [45]. The CNC surface treatment was done by grafting N-morpholino-3-hydroxyazetidinium, N,N-dihexyl-3-hydroxyazetidinium or N,N-diallyl-3-hydroxyazetidinium onto the surface of the nanocrystals and these modified CNCs are hereafter denoted as CNC-Morph-OH, CNC-diHexyl-OH and CNC-diAllyl-OH, respectively. The adopted grafting scheme was a further improved version of a method described in Sahlin et al., 2018, based on a procedure outlined by Chattopadhyay, Keul, & Moeller, 2012 [46]. In the present study, the methylation of the azetidinium salts was omitted but the rest of the azetidinium salt synthesis was based on the description by Sahlin et al., 2018. The hydroxyazetidinium salts were mixed with the aqueous CNC suspension (0.1 mol

equiv per anhydrous glucose unit) in a round-bottomed flask and stirred vigorously. When a good mixing of the salt and CNC had been achieved, the mixture was heated to 90 °C and stirred for 22 h. The reaction mixture was then allowed to cool to room temperature and subsequently washed with acetonitrile and ethanol, and finally deionized water using repeated centrifugation steps.

4.1.4 Poly(ethylene acrylic acid)

The matrix material in these studies was an insoluble aqueous dispersion of EAA containing 20 wt% solids content obtained from BIM Kemi AB, Sweden. The milky white dispersion had a pH of 9.7, a melting point of 88 °C, a melt flow rate of 36 g/10 min (ISO 1133, 190 °C, 2.16 kg) and was neutralized to its ionomer form, all according to the supplier. The polymer had an acrylic acid content of 15 %.

4.2 Characterization Methods

4.2.1 Scanning Electron Microscopy

In paper I, the morphology of the dried CNF paste was obtained via Scanning Electron Microscopy (SEM) using LEO ULTRA 55 FEGSEM. The samples were gold sputtered for 80 s at 10 mA to obtain a 10 nm thick gold coating layer.

4.2.2 Atomic Force Microscopy

In paper I, measurements were performed on a 10 ppm dried suspension of the CNF in tapping mode in air using the Nanoscope IIIa with a Micro Masch silicon cantilever NSC 15 with a type G scanner (Digital Instruments Inc.). For paper II, the dimensions of the CNC were obtained from a previous paper where 200 CNC crystals were measured by atomic force microscope (AFM) [47].

4.2.3 Fibre Analysis

In paper I, the length and width of the CNF was characterized using a Kajaani FS300 fibre analyser (Metso Automation, Finland) according to T271 Tappi standard. Fibre length and width were taken as the average of 30000 fibre pieces. The fibres based on the centre line length was used for the estimation of the amount of fines.

4.2.4 ζ- potential

In paper II, all the CNC samples were diluted to 0.05 wt.% dry content before ion exchange and then had their ζ-potential measured at 25 °C using a Zetasizer Nano ZS (Malvern Instruments, UK) based on the Laser Doppler Velocimetry technique. The light source was a 50 mW diode-pumped solid-state laser with a wavelength of 532 nm and a DTS1070 disposable folded capillary cell was used. The samples were run in triplicates and before each run it was stabilized for 120 s. This method was used to confirm the grafting on the CNCs.

4.2.5 Dynamic Light Scattering

The Malvern Instruments Zetasizer ZEN3600 was used to measure the hydrodynamic diameter of the milky white EAA dispersion at room temperature by diluting it to 0.01 wt.% with deionized water and sonication.

4.2.6 Rheology

In paper I, the rheological properties of the CNF suspension (dry content of 10 wt.%) and CNF-EAA suspensions with a dry CNF content of 0.7 wt% and 1.8 wt% (total suspension dry content was 4.6 wt.% and 2.3 wt%, respectively) were measured using an Anton Paar MCR702, Twin-drive shear rheometer (Graz, Austria). Oscillatory shear strain (0.1 – 100 % strain at 1 Hz), steady shear flow (0.1 – 100 s^{-1}) measurements and temperature sweeps between 27 to 90 °C at 1 Hz and a strain amplitude of 0.2 % was used to characterize these suspensions in their linear viscoelastic range. A cone-plate geometry was used for the oscillatory shear strain and steady flow measurements while a parallel-plate fixture, with silicone oil to reduce the evaporation of water, was used for the temperature sweep. In paper II, the rheological properties of the CNC under consideration had previously been investigated [44].

4.2.7 Composite Preparation

The EAA matrix was reinforced by four different types of cellulosic reinforcement; CNF (Paper I), reference pulp fibres (Paper I) and modified/unmodified CNC (Paper II). In paper I, all the composite samples were prepared via wet mixing method using an L&W pulp disintegrator Lorentzen & Wettre, Sweden at 2900 rpm for 20 mins, while in paper II an IKA T25 digital Ultra Turrax was used at 7900 rpm for 6 mins. In both the papers, the suspensions containing the EAA dispersion, the cellulosic reinforcement and water (total water content of 96 ± 1 %) were mixed at room temperature. These suspensions were dried in room temperature before being compression moulded into plates at 105 °C and 500 bar using a Bucher–Guyer KHL 100, Switzerland. Here, the compression moulding cycle time was approximately 10 minutes.

The composites reinforced with CNF had a final dry CNF loading content from 10 – 70 vol.% whereas the pulp reinforced reference composites had three loading contents of 20, 50 and 70 vol.% pulp fibres.

However, the CNC reinforced (modified and unmodified) samples had a weight fraction of 0.1, 1 and 10 wt.% in the final composite which corresponds to 0.06, 0.6 and 6.8 vol.% respectively. Furthermore, a 10 wt.% (6.8 vol.%) pH neutralized modified CNC reinforced sample was also prepared in the work in Paper II by similar method as mentioned above but a lower compression pressure and cycle time of 5 bar and 5 minutes, respectively, were used.

4.2.8 X-ray Tomography

In paper I, the dispersion of the composite was evaluated by making a 3D interpretation of the internal structure of composites using a Zeiss Xradia XRM520 X-ray tomograph. The scanned composites volume were reconstructed into voxels of the size 1 μm^3. Since 16-bit gray scale can be related to density of the material, a voxel gray scale was generated using the ImageJ software. On the basis of surface reconstructions, the 3D image of the composite internal structure was made in 3D slicer.

4.2.9 Kofler Bench

In Paper II, the visual assessment of thermal stability of all the 10 wt.% CNC composites was conducted using the Kofler bench, which provides a heat gradient over the length of the bench. In order to determine the temperature at which discolouration occurred, the samples were placed at 120, 130, 140, 150 and 160 °C for 8 minutes. Similarly, a comparison was also made between the pH neutralized 10 wt.% CNC-diAllyl-OH and the 10 wt.% untreated CNC composite.

4.2.10 Thermogravimetric Analysis

In paper II, to assess the onset of thermal degradation of the CNC as well the 10 wt.% unmodified/modified CNC composites, a thermal gravimetrical analysis was performed. A TGA/DSC 3+ Star system from Mettler Toledo, Switzerland was used to subject the sample, of approximately 10 mg, to a heating ramp of 5 °C/min between 25 and 550 °C under nitrogen at a flow rate of 50 mL/min. This method was used to confirm the grafting on the CNCs.

4.2.11 Dynamic Mechanical Thermal Analysis

In both the papers, the dynamic-mechanical properties were measured using a Rheometrics RSA II at a frequency of 1 Hz. In paper I, an initial strain sweep was performed on the samples to assess the linear viscoelastic range followed by a temperature sweep at a strain amplitude between 0.1 and 0.15 % according to sample between -80 to 110 °C. Whereas in paper II, specimens were subjected to a basic strain, in tension, of about 0.15 % which was maintained throughout the strain sweep test. The strain sweep test was an applied sinusoidal deformation ranging from 0.03 to 0.14 % at room temperature.

4.2.12 Differential Scanning Calorimetry

The thermal transitions and the crystallinity of the composites were evaluated using a Perkin-Elmer DSC7. The measurements were recorded at a scan rate of 10 °C/min from 10 to 250 °C for the CNF based composites (Paper I) and -20 to 150 °C for the CNC based composites (Paper II) in a nitrogen atmosphere. For the CNF composites, a second temperature scan was used whereas this was omitted for the CNC based composites. The sample mass used was approximately 10 mg and the crystallinity (Xc) was evaluated as

$$X_c = \frac{\Delta H_c}{w_{EAA}\Delta H_o} \quad (1)$$

where ΔH_c is the specific heat of fusion of the composite, w_{EAA} the weight fraction of EAA and ΔH_o the specific heat of fusion for polyethylene crystals taken as 277.1 J/g [48].

4.2.13 Tensile Mechanical Testing

In both the papers, the mechanical properties of the composites were evaluated according to the ISO 527-3 standard. Prior to testing, the dumb-bell shaped samples were conditioned for at least 48 hours at 23 ± 2 °C and 50 ± 5 % relative humidity (RH). The samples had a thickness of approximately 1 mm, gauge length of 20 mm and gauge width of 4 mm. In paper I, a Zwick Z1/ Roell with a 1 kN load cell, grip separation of 40 mm and a crosshead speed of 6 mm/min was used along with a Zwick Eye UI 1540M video extensometer. A pre-load of 0.1 N was applied on all samples before measurement. The tensile measurements were made at 23 ± 2 °C and 50 ± 5 % RH in a condition room. In paper II, a Zwick/Z2.5 tensile tester with a 500 N load cell was used for testing at room temperature.

The Cox-Krenchel model was used to compare the tensile modulus according to eq.2.

$$E_C = \eta_d \left(1 - \frac{\tanh(\beta a)}{\beta a}\right) \phi E_f + (1 - \phi) E_m \qquad (2)$$

where

$$\beta = \sqrt{\frac{E_m/(1+\nu_m)}{r^2 E_f \ln(\frac{R}{r})}} \qquad and \qquad R = \sqrt{\frac{\pi r^2}{4\phi}}$$

E_m, E_f and E_c denote the the elastic moduli of the EAA matrix, the cellulose fibre and the composite, respectively [49, 50]. E_m was measured to be 0.29 GPa and E_f was set to 21 GPa for cellulose fibres [51] and 32 GPa for the CNF [52]. The ϕ is the volume fraction of cellulose and η_d is the orientation factor which was assumed to be 3/8 corresponding to a random in-plane fibre orientation [50]. The Poisson ratio, ν_m, for the EAA matrix was assumed to be 0.3 and r is the fibre radius. Fibre dimensions were taken from the results of the fibre analysis. Furthermore, in paper I, the effective stiffness of CNF ($E_{f,l}$) was calculated using the Halpin–Tsai model as mentioned previously [53].

$$E_{f,1} = \frac{\frac{3}{8}\left(E_C - \frac{5}{8}E_T\right) - E_m(1-\phi)}{\phi} \qquad (3)$$

where

$$E_T = E_m \left(\frac{1+2\eta\phi}{1-2\eta\phi}\right) \quad and \quad \eta = \left(\frac{E_{f,t} - E_m}{E_{f,t} + 2E_m}\right)$$

The transverse fibre modulus ($E_{f,t}$) in eq. 3 was set to 15 GPa [54].

5
RESULTS AND DISCUSSION

5.1 Characterization of Cellulose and EAA

The raw materials in paper I, were characterized using AFM, SEM, fibre analysis techniques and DLS to determine their morphology. The results on CNF used in this study revealed that it had a wide distribution of fibre/fibril sizes and appeared to be a mixture of nanofibrils, microfibrils and fibres. As seen in the microstructure of the CNF, the smallest fibrils had diameters in nanometres (see figure 6a) whereas as a large amount of fibril diameters were in the micrometre scale (see figure 6b). Furthermore, the fibre analysis also showed the presence of fibre remnants which suggest an incomplete fibrillation process. The fibre remnants of the CNF when compared with the reference pulp fibres where actually shorter in length and the higher amount of fines content in the CNF suggest a higher degree of fibrillation compared to the highly beaten pulp, (see table 2). However, it was not possible to determine the relative content of the fibrils and fibres due to the limitation of size range of each analysis technique used. This led to choosing the dimensions from Table 2 for modelling the tensile modulus of the CNF and pulp based composites in paper I.

As for paper II, the CNC had an average width and length 211 ± 114 nm and 6.0 ± 1.5 nm, respectively [47]. No further characterization was made on these unmodified CNC due to the extensive characterization in a prior paper [44]. For the modified CNC, the grafting was confirmed through ζ-potential measurements where the surface charge of the CNC reduced with modification suggesting that grafting of the azetidinium salts were successfully, see in Table 3. However, when compared to the other modifications, the CNC-Morph-OH had the lowest degree of substitution.

Table 2: Fibre analysis of CNF and pulp

Cellulose Type	Length (mm)	Width (μm)	Fines (%)
CNF	0.34	18.4	78
Pulp	1.36	24.4	11.9

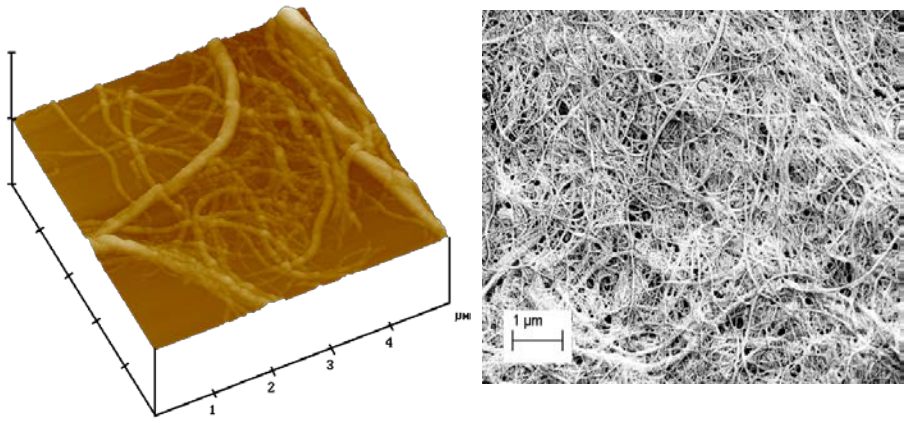

(a) **(b)**

Figure 6: Micrograph of dried cellulose nanofibrils as seen with **(a)** AFM and **(b)** SEM.

Table 3. The ζ-potential (Standard deviation in parentheses) of ion exchanged CNC at a concentration of 0.05 wt%.

Type of CNC	ζ-potential (mV)
CNC-unmod.	-71.7 (2.0)
CNC-Morph-OH	-40.9 (1.1)
CNC-diHexyl-OH	-32.5 (2.5)
CNC-diAllyl-OH	-31.0 (2.1)

Finally, for the EAA dispersion Dynamic Light Scattering was used to determine the particle size, which was 50 nm, and this size was smaller than most dispersions used in other works to prepare CNF composites e.g. Larsson et al., 2012 [34].

5.2 Rheology of EAA-CNF suspensions

In order to assess the effect of varying CNF content in the EAA-CNF suspension, the rheological properties of CNF paste (10 wt.% dry content) and EAA-CNF suspensions (0.7 wt.% and 1.8 wt.% CNF respectively with 96 ± 1 % water) were measured. The suspensions exhibited a prominent elastic character as seen by the higher shear storage modulus (G') compared to the shear loss modulus (G''), see figure 7. As expected, the suspensions also showed an increase in G' with increasing CNF content. Furthermore, an increase in the critical strain (from 1.1 % to 2.3 %), the strain at which transition from linear viscoelastic to nonlinear region occurs, was observed with decreasing CNF concentration due to addition of EAA and

excess water [55]. However, in contradiction to other results e.g. Naderi, Lindström, & Sundström, 2014, no influence of CNF concentration was observed on the slope of the curve in the shear thinning region [57].

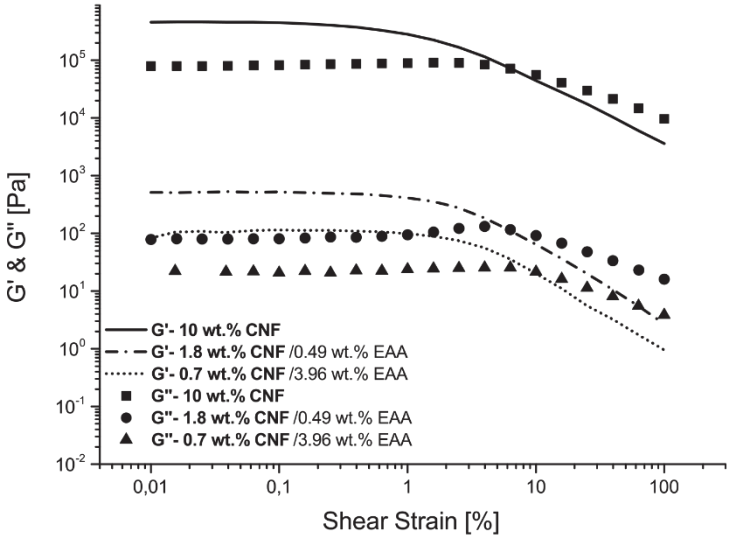

Figure 7: The dynamic shear storage modulus (G', solid line) and the shear loss modulus, (G'', dashed line) as a function of shear strain.

The steady shear viscosity showed a shear thinning behaviour in agreement with earlier works [58]. However, due to slippage the viscosity of the CNF paste could not be measured at shear rates above 5 s^{-1}.

The temperature ramp performed on the EAA-CNF suspensions had limitations in temperature range, as expected with the water content of 96 %. Among the two CNF-EAA suspensions, only the CNF-EAA suspension with 0.7 wt.% CNF and 3.95 wt.% EAA showed a G' peak at 59 °C, which was close to the first melting point of EAA, suggesting a morphological change in the EAA dispersion which was noticeable at this particular concentration.

5.3 Composite Dispersion

In order to assess the dispersion and the microstructure of the composites in paper I, micro-tomography images of EAA-CNF-20 and EAA-Pulp-20 composite are compared. The structure was reconstructed with a voxel size of 1 μm^3 and based on the number of volume elements against voxel gray scale, related to material density, three phases could be distinguished, see figures 8 and 9. The phase with the highest voxel density was assumed to correspond to the cellulose fibres and fibrils. In the case of EAA-CNF-20 (see figure 8a) this represented a very small fraction, about 2.5 vol.%, which suggested that the medium density phase (96.9 vol.%) was a mixture of the matrix (EAA) and CNF which fell below the resolution limit of the instrument (1 µm/voxel). The same can be said for the highly beaten pulp fibres (see figure 9a) which showed a volume fraction of 13 % in the high density phase. The third and final phase that was distinguishable was the low density phase which appeared around the cellulose surface and in the lumen (see figure 8b and 9b). This would likely represent the interphase between the matrix and the reinforcement or voids.

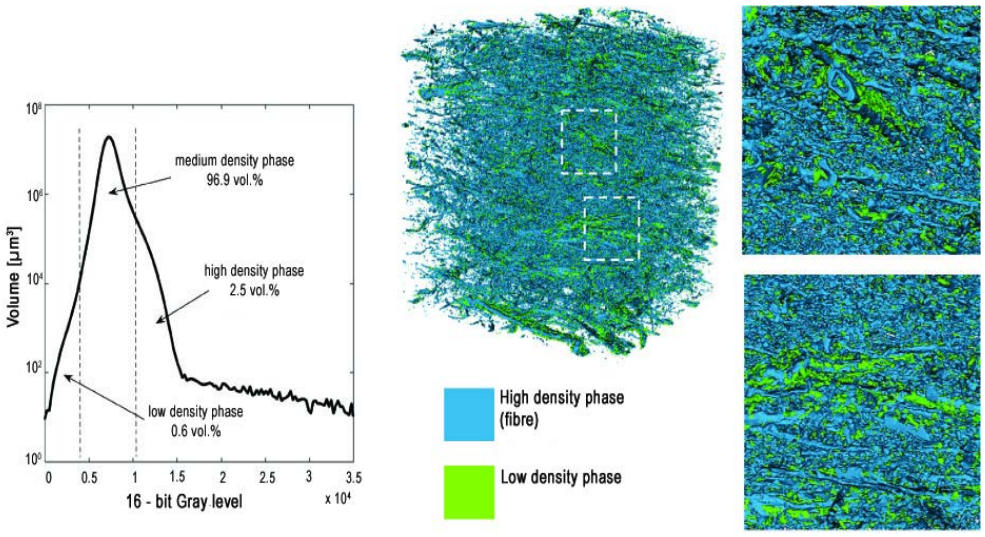

(a) **(b)**

Figure 8: EAA–CNF-20 ***(a)*** X-ray microtomography data showing three density phases for the EAA–CNF-20 material, ***(b)*** 3D reconstruction of the (blue) high density fibre phase and the (green) low density phase.

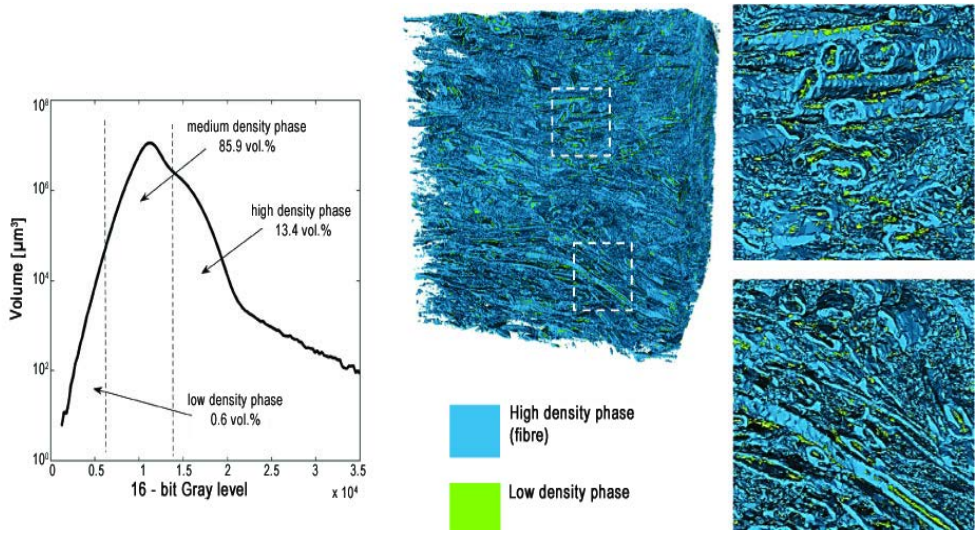

(a) **(b)**

Figure 9: EAA–CNF-20 **(a)** X-ray microtomography data showing three density phases for the EAA–Pulp-20 material, **(b)** 3D reconstruction of the (blue) high density fibre phase and the (green) low density phase.

5.4 Thermal Properties and Crystallinity

5.4.1 Thermal Stability of CNC

In paper II, the grafting was verified through the thermal stability of the modified CNC using thermogravimetric analysis. It showed that the onset of degradation of the grafted CNC increased by almost 100 °C when compared to its unmodified counterpart, as shown in Table 4 and Figure 11b. This would likely be due to the removal of acidic hydrogen of the sulphate half ester which prevents catalytic degradation [44, 59]. In order to confirm the thermal stability of CNC in composites, the 10 wt.% CNC composites were studied with the help of TGA along with a visual assessment using the Kofler bench.

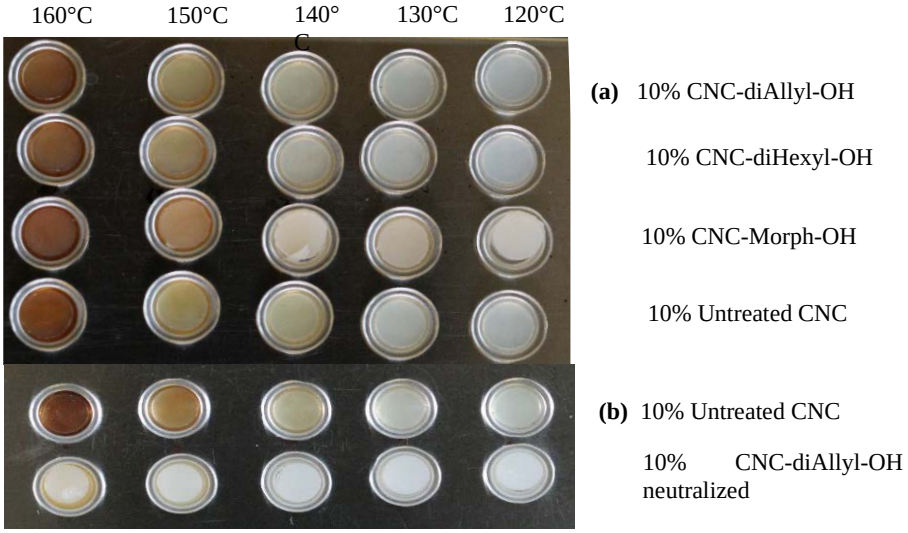

Figure 10: **(a)** Visual appearance of the composites containing 10 wt.% CNC after exposure for 8 minutes. **(b)** Visual appearance of the composites containing 10 wt.% untreated CNC and 10 wt.% CNC-diAllyl-OH from the pH neutralized system after exposure for 8 minutes. All samples from right to left 120, 130, 140, 150 and 160 ˚C.

As seen in figure 10a, the composites placed on the Kofler bench for 8 minutes at 120, 130, 10, 150 and 160 °C showed a change in colour already at 150 °C and at 160 °C all the composite samples were brown. Interestingly, the modified CNC based composites behaved similar to the unmodified CNC based composite when it came to visual assessment of thermal stability and the TGA results confirmed this (see figure 11). However, when a pH-neutral 10 wt.% composite containing CNC-diAllyl-OH was studied, no significant colour change was observed, as seen in figure 10b, and this was also confirmed by the TGA (see figure 11a). Even though the CNC samples showed thermal stability up to 250 °C (see figure 11b), the composites did not replicate this behaviour (except for pH-neutralized 10 wt.% CNC-diAllyl-OH based composite). This explanation can be related to the alkalinity of the EAA dispersion which has a pH of 9.7. It is known in organic chemistry that the chemical stability of the sulphate diester, which acts as a good leaving group in the presence of nucleophiles (hydroxides and carboxylates), is poor in alkaline environments. Due to this, the azetidinium groups which are grafted will not likely impart the thermal stability. However, in order to confirm that the grafting remained on the composite at the temperature used during composite

preparation, an indirect method was used wherein a sample of CNC-diAllyl-OH, adjusted to pH of 9.7, was prepared at 105 °C and 5 bar. These samples showed no difference in the TGA curve before and after the heating suggesting that the degrafting occurs at higher temperatures for these composites.

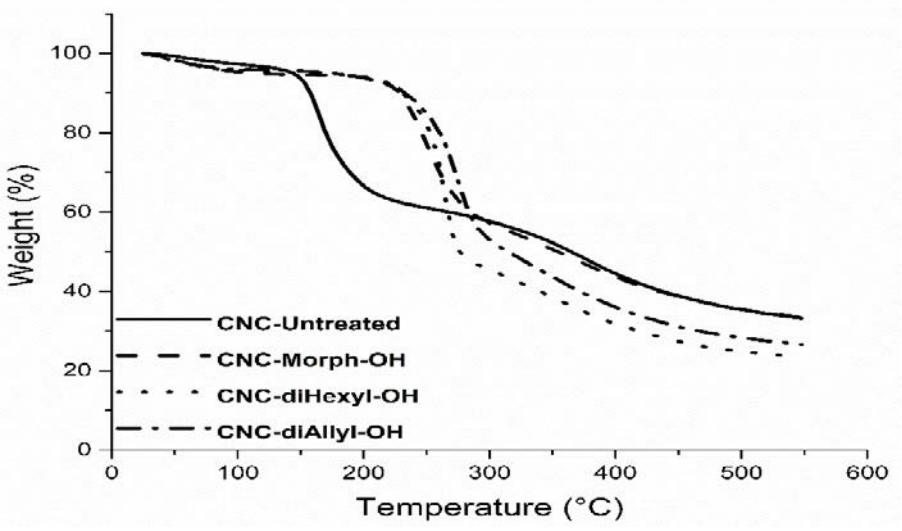

(a)

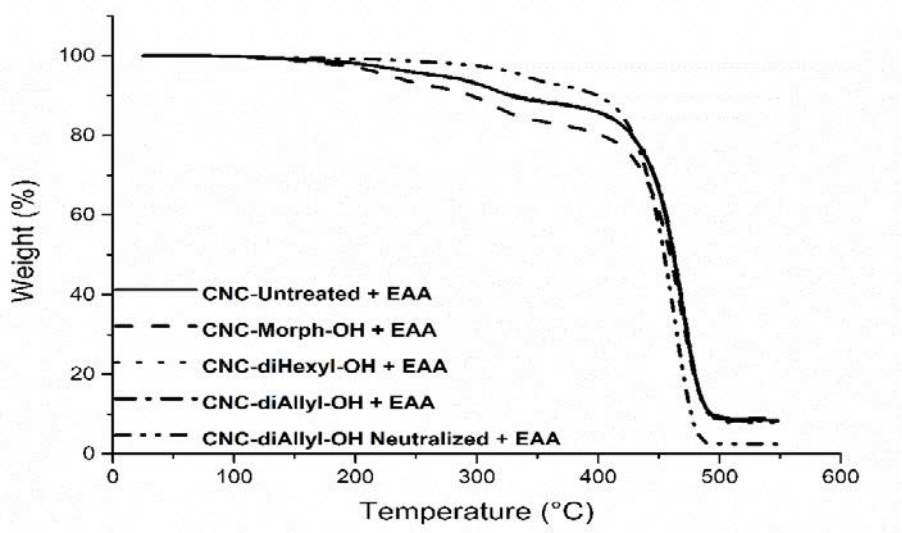

(b)

Figure 11: Thermogravimetric curves showing the thermal degradation of **(a)** untreated and surface-modified CNC and **(b)** the composites containing 10 weight-% of unmodified CNC, surface-modified CNC and a neutralised mixture of EAA and CNC-diAllyl-OH

Table 4. The onset of thermal degradation and the weight percentage of residual char at 550 °C.

Type of CNC	T_{onset} (°C)	Residual char (%)
CNC-unmod.	157	32
CNC-Morph-OH	224	33
CNC-diHexyl-OH	248	23
CNC-diAllyl-OH	247	27

5.4.2 Differential Scanning Calorimetry

The influence of the nanocellulosic reinforcements on the thermal transitions and crystallinity of the semi-crystalline EAA was investigated. As seen in figure 12, EAA showed the presence of multiple melting endotherms, the first being at 51 ± 2 °C and the second at 87 ± 1 °C. However, after cooling at 10 °C/min and subjected to a second heating, a prominent peak at 87 ± 1 °C was observed and this could be related to the melting of non-isothermally crystallized EAA [23]. The low temperature melting peak observed can be associated with time dependent crystallization, which is seen for neutralized ionomers like EAA, of thin crystals which occurs at room temperature after the primary crystallization [24]. The peak position remained similar with the addition of CNF and no significant changes were observed in crystallinity, as seen in Table 5, even though previous works have shown that the crystallinity can either increase or decrease with addition of CNF [28, 60, 61].

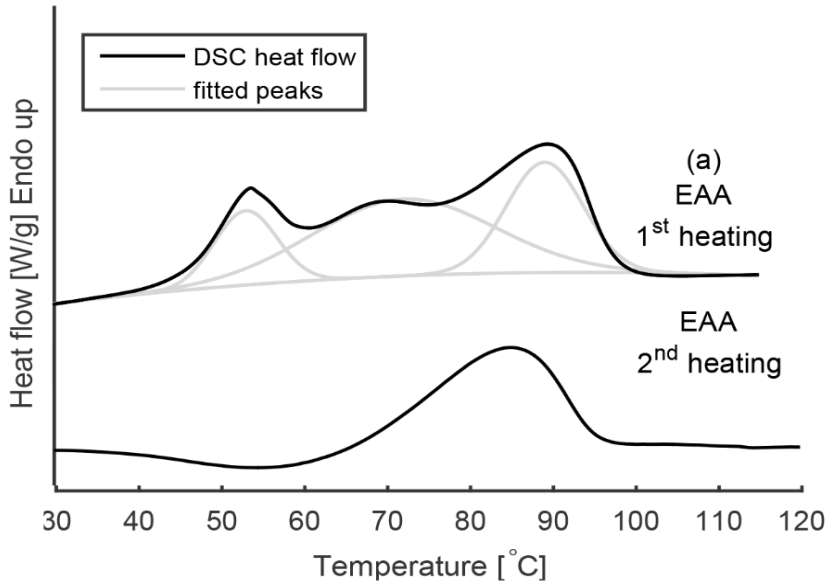

Figure 12: Thermograms of the first and second heating scans for a neat compression moulded EAA composite.

Similarly, no significant changes were observed in matrix crystallinity for the CNC based composites. It is important to note that, in both the papers, the improvements in mechanical properties cannot be attributed to the changes in the composite crystallinity.

Table 5. The thermal properties of cellulose-EAA composites.

Sample	Cellulose	$T_{m1} = 51 \pm 2\ ^{o}C$		$T_{m2} = 87 \pm 1\ ^{o}C$
	vol%	wt%	X_{c1} (%)	X_{c2} (%)
EAA	–	–	3	16
EAA–CNF-10	10	15	2	15
EAA–CNF-20	20	28.4	6	14
EAA–CNF-30	30	40.5	5	12
EAA–CNF-40	40	51.4	3	15
EAA–CNF-50	50	61.3	5	12
EAA–CNF-60	60	70.4	5	14
EAA–CNF-70	70	78.8	6	10
EAA–Pulp-20	20	28.4	7	12
EAA–Pulp-50	50	61.3	4	10
EAA–Pulp-70	70	78.8	3	9

5.4.3 Dynamic Mechanical Thermal Analysis

The effect of sinusoidal strain on the composites were analysed in both the papers. In paper I, a constant sinusoidal strain was applied over a range of temperature as shown in figure 13. Here, the DMTA was used to discern the thermal transitions of the composite and the effect of CNF addition on them. The transitions were recognised through the variation of the dynamic storage modulus and the loss factor of the composite. The three transitions observed were distinguished as, the glass transition temperature of the matrix (at -39 ± 4 °C), first melting peak, T_{m1}, of the EAA matrix at 55 ± 5 °C, comparable to the DSC data (see figure 12) and finally the second melting peak, T_{m2}, which was evident through the loss factor curves (see figure 13b) up to samples containing 30 vol.% CNF. As seen in figure 13, the addition of CNF increased the magnitude of the storage modulus (E') not only below glass transition but also after the first melting peak at 55 °C. Furthermore, the addition of CNF reduced the drop of E' after T_{m1} suggesting an improvement in the thermo-mechanical properties. The transitions observed became evident with increasing CNF content and were insignificant above 40 vol.% CNF.

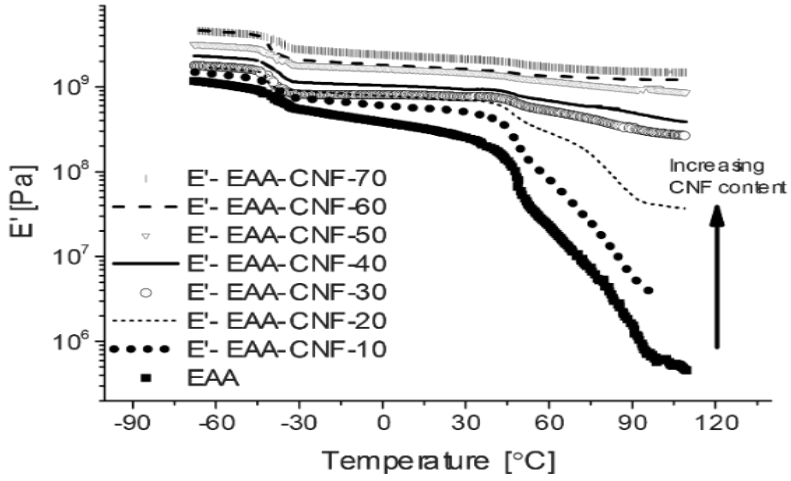

(a)

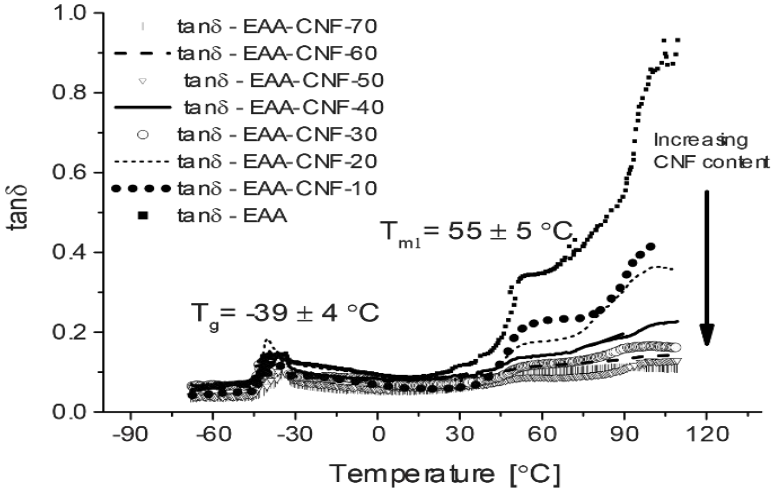

(b)

Figure 13: **(a)** Storage Modulus (E') and **(b)** loss factor (tan δ) of CNF-EAA composites measured at a constant strain amplitude between the temperatures -80 to 110 °C at a frequency of 1 Hz, a heating rate of 3 °C/min.

In Paper II, the CNC composites were subjected to a range of sinusoidal strain while maintaining a constant basic strain of 0.15 % on them. These samples were then subjected to strain sweep tests in order to predict the interaction of the surface modified CNC with the matrix through the mechanical loss factor values. Nielsen showed that the effect of surface treatment on the mechanical loss factor could be related to polymer-filler friction or poor adhesion between reinforcement and the matrix [62]. Previous work have described the formation of an interphase region close to the reinforcing/filler particle with properties different from the bulk polymer [63]. This interphase region can be described to have an influence on the mechanical loss factor written as

$$\tan \delta_c = v_f \tan \delta_f + v_i \tan \delta_i + v_m \tan \delta_m \qquad (4)$$

where the subscripts f, i and m refer to the filler, the interphase region and the polymer matrix, respectively, and v denotes the corresponding volume fractions of the components. Even though the above equation maybe an oversimplification of the loss factor of the composite it can

intuitively be useful to predict that the loss factor increases if the interphase is weak due to the increase in losses and vice versa if the interphase is strong [63].

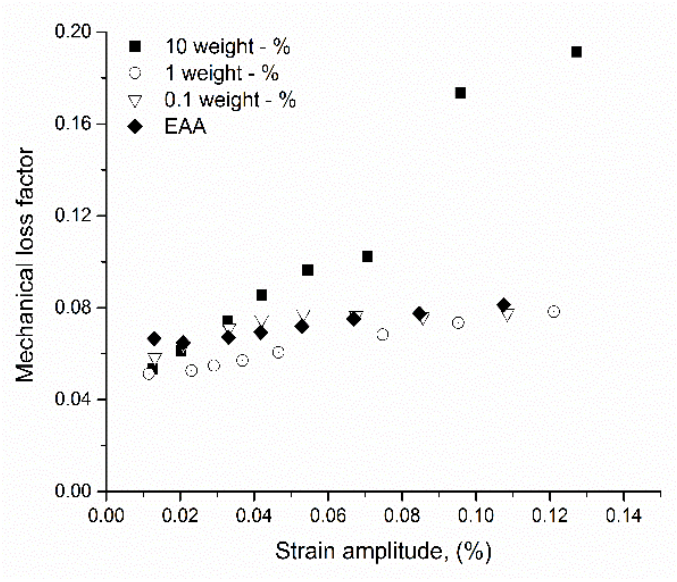

(a)

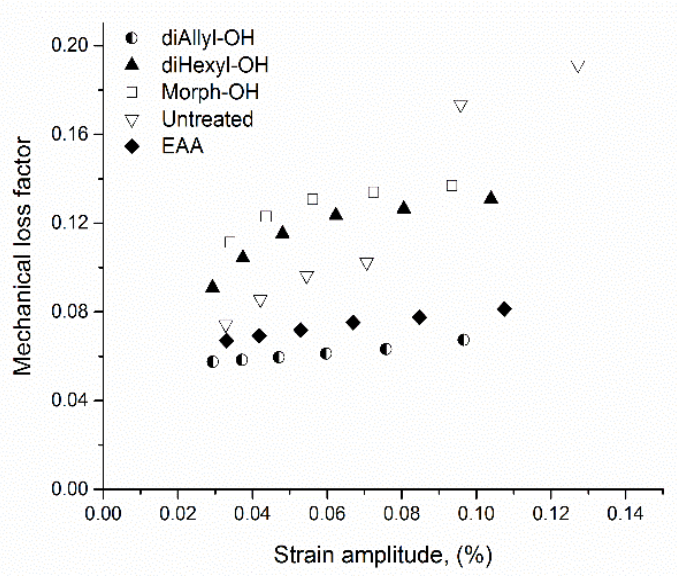

(b)

Figure 14: Mechanical loss factor as a function of applied strain amplitude on composites containing **(a)** 0 (EAA), 0.1, 1 and 10 wt..% untreated CNC and **(b)** EAA and 10 wt.% unmodified and modified CNC.

Based on the above model, trends could be observed for the CNC based composites with different loading contents and surface modification, as seen in figure 14. For the unmodified CNC composites at low loading contents (0.1 to 1 wt%), the samples were insensitive to variation in strain amplitude and not much variation in the loss factor (tan δ_C) was observed when compared to the matrix material. At a concentration of 10 wt.% the loss factor was more sensitive to the applied strain amplitude and increased with increasing strain amplitude which could indicate a probable loss of adhesion between CNC and the matrix [62]. Overall, the

highest CNC concentration results were the clearest to suggest the effect of surface treatment. From the figure 14b, it could be observed that the samples with 10 wt.% modified CNC showed the least sensitivity to the strain amplitude even though the CNC-Morph-OH and CNC-diHexyl-OH had higher loss factor values at lower strain amplitudes. Furthermore, the composite with 10 wt.% CNC-diAllyl-OH exhibited tan δ_C values lower than that of the matrix and this is not unrealistic if the adhesion between the reinforcement and CNC is good since the CNC should have tan δ as low as 0.01 [64]. The tan δ_C values of the modified composites suggest a strong and flexible interphase region, especially for CNC-diAllyl-OH as it exhibited the highest yield strength at the highest CNC concentration (see Table 7).

5.5 Tensile Mechanical Properties

The EAA matrix used in both the studies was a rather ductile polymer with a defined yield point at around 13 %. However, with the addition of CNF and CNC ($\geq$ 10 wt.%) the ductility was lost significantly. In paper I, the distinct yield point was replaced by a gradual increase in stress until fracture relating to the rearrangements of the entangled fibril network due to deformation [65, 66]. The effect of reinforcement increased with increasing CNF content and this was evident from the modulus (E) and strength (σ_b) of the composites which increased from 0.3 GPa and 24 MPa, respectively for neat EAA to 6.2 GPa and 83 MPa, respectively for 70 vol.% CNF content. This represents a stiffening factor of 21 and a strengthening factor of 3.5. Interestingly, the pulp-EAA based composites were stiffer and had similar strength as the CNF based composites at 20 vol.% loading but above this concentration the CNF based composites had higher values which was expected due to the higher aspect ratio and modulus of cellulose fibrils than pulp fibres [40, 52]. Furthermore, a stiffening threshold, also observed by other works [28, 34], at around 20-30 vol.%, was observed for the CNF-EAA composites leading to a rise in the stiffness and strength of the composite (see Table 6).

This improvement in properties could be due to formation of entanglements in the fibril network at this point of percolation. However, the strain at break (ε_b) on the other hand reduced with increasing CNF content, as expected, with the highest and lowest value being 32 % and 5 % for the 10 vol.% CNF-EAA composite and 60 vol.% CNF-EAA composite, respectively. The pulp-EAA composite always had a lower ε_b than the CNF based composites, implying that the CNF composites had a better stress transfer, fibril mobility and higher resistance to deformation. The mechanical properties of these composites could likely be further improved if the voids near the surface (see figure 8) could be reduced.

In paper II, the tensile properties were evaluated based on the yielding behaviour of the composites rather than ultimate properties and this was possible since the loading contents were low (< 10 wt.%). On the whole, the effect of CNC on the modulus was positive even at the low loading contents. The E increased from 0.3 GPa, for the matrix, to 0.9 GPa for the 10 wt.% unmodified CNC. The yield stress followed a positive trend too with CNC-Morph-OH showing the highest values at low CNC-concentrations and the CNC-diAllyl-OH exhibiting the highest values at the 10 wt.% concentration.

Table 6: Mechanical properties of cellulose-EAA composites

Sample	Tensile Properties			Effective Stiffness
	E (GPa)	**σ_b (MPa)**	**ε_b (%)**	**$E_{f,1}$ (GPa)**
EAA	0.3 ± 0.1	24 ± 1	491 ± 19	-
EAA-CNF-10	0.7 ± 0.1	26 ±1	32 ± 5	9.4
EAA-CNF-20	1.6 ± 0.1	37 ± 1	14 ± 2	15.9
EAA-CNF-30	3 ± 0.4	57 ± 1	8 ± 1	22.3
EAA-CNF-40	4 ± 0.6	64 ± 12	8 ± 2	21.4
EAA-CNF-50	4.3 ± 0.3	65 ± 5	6 ± 1	19
EAA-CNF-60	5.3 ± 0.6	71 ± 11	5 ± 2	19.3
EAA-CNF-70	6.2 ± 0.3	83 ± 10	8 ± 1	18.6
EAA-Pulp-20	1.8 ± 0.5	35 ± 3	6 ± 1	18.6
EAA-Pulp-50	4.4 ± 1.2	46 ± 5	3 ± 1	19.5
EAA-Pulp-70	4.9 ± 0.2	55 ± 4	3 ± 0.3	13.7

However, no yield point was visible for the brittle unmodified CNC 10 wt.% composite. Importantly, the incorporation of CNC into the matrix caused an increase in the yield stress values which is not usually the case when incorporating rigid fillers into a polymer matrix [62].

The ductility of the composite was seen to increase by modification at low CNC concentrations (0.1 and 1 wt.%), see table 7, and in general this may be attributed to the enhanced interaction between the matrix and the grafted groups, even though the mechanism of interaction was rather complex. In the case of low concentration CNC based composite, the enhanced ductility could be due to the presence of CNC or the interaction between the surface groups themselves and/or with the polymer matrix. This can be plausible at concentration close to the percolation threshold where minor aggregation through OH-interaction of the CNC can be assumed. As for the grafted groups, hydrophobic interactions (dihexyl), π-π interactions (diallyl) and hydrogen bonding (morpholine) can be assumed as means of interaction to enhance properties. The largest improvement of properties was achieved by morpholine at low CNC concentrations implying the presence of interactions either between CNC or CNC and the matrix since the morpholine has the largest tendency among the modifications to interact with carboxylate groups of the matrix.

Table 7: Mechanical properties of CNC-EAA composites.

Sample	**Modulus** (MPa)	**Yield stress** (MPa)	**Yield strain** (%)	**Failure stress** (MPa)	**Failure strain** (%)
0.1 % CNC-Morph-OH	294 (28)	14.1 (0.5)	10.4 (0.6)	24.3 (0.8)	284 (11)
0.1 % CNC-diAllyl-OH	237 (25)	12.1 (1.0)	12.2 (0.4)	21.2 (1.3)	276 (11)
0.1 % CNC-diHexyl-OH	249 (24)	12.8 (0.6)	12.0 (0.8)	23.5 (1.4)	288 (15)
0.1 % untreated CNC	270 (13)	13.5 (0.3)	11.4 (0.8)	24.5 (0.7)	278 (6)
1 % CNC-Morph-OH	367 (22)	15.2 (0.6)	10.2 (0.4)	23.4 (1.3)	252 (10)
1 % CNC-diAllyl-OH	314 (21)	14.1 (0.6)	11.0 (0.5)	22.9 (1.0)	261 (10)
1 % CNC-diHexyl-OH	295 (16)	14.1 (0.4)	11.7 (0.9)	23.7 (1.2)	267 (10)
1 % untreated CNC	353 (18)	15.3 (0.5)	9.9 (0.2)	25.3 (1.7)	246 (7)
10 % CNC-Morph-OH	678 (46)	15.1 (0.4)	7.5 (0.4)	14.2 (2.3)	11 (10)
10 % CNC-diAllyl-OH	864 (32)	21.1 (0.7)	8.2 (0.8)	19.7 (0.8)	31 (22)
10 % CNC-diHexyl-OH	678 (21)	17.9 (0.4)	8.6 (0.7)	16.5 (1.0)	28 (15)
10 % untreated CNC	921 (64)	-	-	21.9 (0.9)	6 (1)
EAA	322 (5)	15.1 (0.6)	9.6 (0.6)	25.8 (1.2)	255 (6)

However, at 10 wt.% CNC content, the surface area increase drastically and other factors would likely originate. For the diallyl modified CNC, the effect on mechanical properties are stronger compared to the rest of the substituents. The reasons for this needs to be investigated but it is clear that a tough interphase is created in this composite which leads to efficient stress transfer and enhances ductility while still maintaining good stiffness and yield strength.

5.5.1 Estimation of Composite Tensile Modulus (E_c) and Effective Stiffness ($E_{f,1}$)

The Cox-Krenchel model (eq.2) has been used to determine the stiffness of the CNF and pulp based composites over the range of loading content. However, in paper II, the modulus of CNC (E_f) was calculated through Cox-Krenchel and the acquired modulus of the CNC approached 55 - 60 GPa which is in the vicinity of the glass fibres having a value of 70 GPa.

In paper I, the average aspect ratio of the fibril that was entered in eq.2 was based on the data obtained from the fibre analysis (see Table 2) which means that the pulp fines and cellulose fibrils were neglected and this would mean less accurate modelling results. However, the model was rather accurate for the CNF based composite, see figure 15a. The pulp-EAA composite also fitted the model rather well, (see figure 15b). Furthermore, in paper I, the variation of fibril aggregation was discussed based on the effective stiffness ($E_{f,1}$), see eq.3, which provides intuition into fibril aggregation [53]. The $E_{f,1}$, (see Table 6), varied from a maximum of 22.3 GPa at 30 vol.% CNF to 18.6 GPa for 70 vol.% CNF, which indicates a minor change in dispersion at high loading contents.

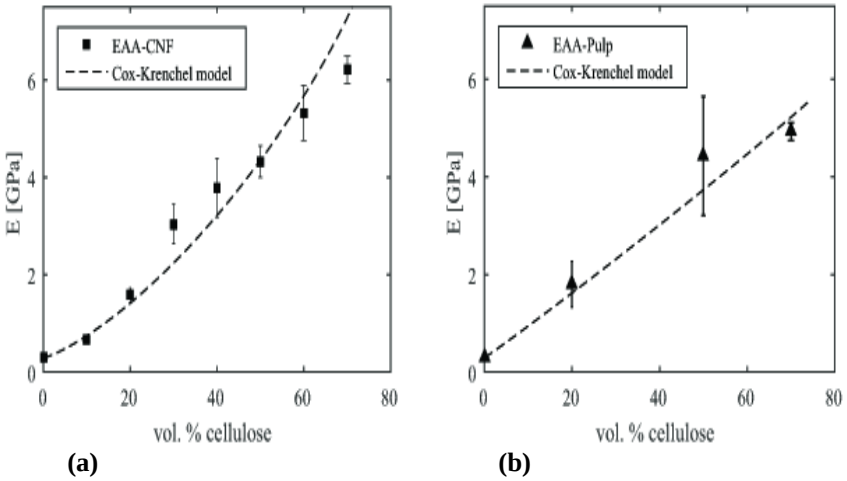

Figure 15: The Cox-Krenchel model predicted for the elastic modulus of **(a)** CNF-EAA composite and **(b)** Pulp-EAA composites.

6
CONCLUSIONS

The work indicated some benefits with using the water-assisted mixing method compared to dry mixing, for preparing better dispersed thermoplastic composite reinforced with CNF or CNC. The excess of water in water-assisted mixing benefited in allowing for dispersion of suspensions that, after drying, could provide composites with high nanocellulose content. The results also indicated the possibility of these materials to be used as composites by themselves or be used as the master-batch in order to produce compounds for large-scale melt shaping processes, such as extrusion and injection moulding. For such large scale processes the material is required to flow efficiently which seems difficult with the composite compounds produced, especially with the higher nanocellulose concentration studied. Hence, further work is needed to obtain high nanocellulose content compounds with good dispersion and reasonable flowability. The further work may include studies on reducing the network of nanocellulose system by using a lower aspect ratio reinforcement and use of other additives.

The addition of CNF substantially improved the thermo-mechanical and tensile properties of the composites produced. At the highest CNF content studied, which was 70 vol.%, the tensile stiffness of the composites was measured to 6 GPa, which was 21 times the stiffness of EAA. This stiffness was however similar to that of the pulp reinforced composites, which had a stiffness of about 5 GPa at 70 vol.% pulp contents. The main difference between the composites reinforced with CNF and pulp was in the tensile strength where the CNF composites at 70 vol.% had a value of 84 MPa compared to the substantially lower value of 55 MPa of the pulp-based composites. The elongation at break for the CNF composites was significantly higher than that of the pulp reinforced composites at similar concentrations. The composites produced did not exhibit a particular trend in crystallinity, suggesting that the changes in properties seen were solely due to the reinforcements.

The CNC was successfully grafted with hydroxyazetidinium salts onto the sulphate ester groups of the CNC, as confirmed by monitoring the surface charge of the CNC using ζ-potential measurements and their thermal degradation behaviour. Assessment of the thermal stability with TGA showed that the onset of thermal degradation of the modified CNC was improved by 100 °C by grafting, but the same was not repeatable in the composites made of modified CNC reinforced ethylene acrylic acid copolymer. The reason for the poor thermal stability of the composite was related to the alkalinity of the EAA dispersions used in the composite preparation which resulted in the degrafting of the functional groups on the CNC at higher temperatures, at about 150 °C as shown in the assessment of thermal stability studies with TGA. The grafting of the modified CNC was found to be intact at the temperatures used for compression moulding in this study (105 °C).

The mechanical properties were improved with the addition of both modified and unmodified CNC. The modified CNC mostly increased the strain at yield and enhanced the ductility of the composite. The results on the loss factor from the dynamic mechanical tests indicated that the surface modification of CNC could provide an improved interphase between the CNC and the matrix, which may explain the improved ductility obtained.

7
FUTURE WORK AND OUTLOOK

The current work encompasses the compression moulding of nanocellulose as reinforcement in an aqueous dispersed copolymer matrix. From a processing perspective, the next set of studies would involve using the composite material as a master-batch which would be compounded and shaped into a final specimen. The twin screw extruder can be utilized for the purpose of compounding and the shaping could be done either through single screw extrusion or injection moulding. The influence of the processing parameters on the final composite would be interesting to study and also in the meantime address the challenges involved in continuous melt processing, such as problems with aggregation and discolouration which are the most evident.

Furthermore, the nanocellulose aspect ratio used would make an impact on the final properties of the composites produced by melt shaping techniques. Hence, a comparative study on CNF and CNC would be necessary in order to be able to select the appropriate nanocellulose to obtain the most favourable properties after melt processing.

In the present work the CNC modification helped maintain thermal stability and this modification, if altered according to the matrix selected, could help move towards commonly used polymers while still maintaining thermal stability and compatibility. The matrices of interest are low density polyethylene (LDPE) and possibly stiffer matrices like polyamides (PA).

8
LIST OF ABBREVIATIONS

AFM	Atomic force microscopy
SEM	Scanning Electron Microscopy
CNC	Cellulose nanocrystals
CNF	Cellulose nanofibrils
PVA	Polyvinyl Alcohol
PA	Polyamide
TPS	Thermoplastic starch
EAA	Ethylene Acrylic Acid
TGA	Thermogravimetric Analysis
DSC	Differential Scanning Calorimetry
DMTA	Dynamic Mechanical Thermal Analysis
LDPE	Low density polyethylene
GFRC	Glass fibre reinforced composites
CNC-Morph-OH	N-morpholino-3-hydroxyazetidinium
CNC-diHexyl-OH	N,N-dihexyl-3-hydroxyazetidinium
CNC-diAllyl-OH	N,N-diallyl-3-hydroxyazetidinium

9
ACKNOWLEDGEMENTS

I would like to express my sincere gratitude and thanks to my supervisor Antal Boldizar for his support, time and patience while supervising me. I appreciate all the advice and help that I have got from the discussions with you and I hope this will continue. A special thanks for your support towards my extra-curricular activities as well.

The Swedish Foundation for Strategic Research is gratefully acknowledged for its financial support in this project. Borregaard is also acknowledged for providing the samples for the work.

My thanks also to Mikael Rigdahl, Roland Kadar and Jörgen Romild for the discussions and experimental support during these years. Håkan Millqvist and Roger Sagdahl are thanked for their support and patience in the lab while helping me out. I would like to especially thank Johannes Thunberg for all the support, advice, tips and fun facts that he has given me. You have been a friend as well as a mentor and I really appreciate your support. Anna Peterson and Karin Sahlin are also thanked as you have had the patience to discuss even when you were busy. Giada Lo Re and Assaya Boujemaoui are thanked for their help with experimental work.

I would like to acknowledge my co-authors and colleagues from the Department of Chemistry and Chemical Engineering. Thank you for all the energy and time you have put into these work and also thank you for showing patience in explaining the CT-scan measurements (Lars Hammar) and chemistry related topics (especially Johannes, Anna Peterson and Karin Sahlin).

The members (old and new) of the polymer group Erik Stenvall, Tobias Moberg, Maria Klinberg, Kristina Karlsson, and Lilian Forsgren for all your support in teaching (thank you for covering for me) and helping me out whenever I was lost. It has been fun working with you all. The colleagues at the Department of Industrial and Materials Science are thanked for the best possible atmosphere and special thanks to my office mate for keeping the mood jovial and bearing with me.

Finally, I would like to thank my friends and my upgraded family (Appaji, Mami and Dwivarna) for all the support and love. A special thanks to my wife whose love and support means everything to me. Amma and Appa, thank you for believing in me and always being there for me. Anji and Abhirama my precious angels. I would never have gotten here without you all. **HSVJ!**

10
BIBLIOGRAPHY

[1] J. W. Hyatt, ‘Improved method of coating billiard-balls, &c’, US Patent No. 88634, 1869.

[2] R. Geyer, J. R. Jambeck, and K. L. Law, ‘Production, use, and fate of all plastics ever made’, *Sci. Adv.*, vol. 3, no. 7, p. e1700782, Jul. 2017.

[3] K. B. Lindahl, J. Johansson, R. Lidskog, T. Ranius, and J.-M. Roberge, ‘The Swedish forestry model: More of everything?’, *For. Policy Econ.*, vol. 77, pp. 44–55, Apr. 2017.

[4] H. Kargarzadeh, I. Ahmad, S. Thomas, and A. Dufresne, ‘Methods for Extraction of Nanocellulose from Various Sources’, in *Handbook of Nano-Cellulose and Cellulose Nanocomposites*, Alain Dufrsne, Ed. John Wiley & Sons, Incorporated, 2017, pp. 1–50.

[5] European Union, ‘A European Strategy for Plastics in a Circular Economy - SWD(2018) 16 final’, Brussels, 2018.

[6] S. . Joshi, L. . Drzal, A. . Mohanty, and S. Arora, ‘Are natural fiber composites environmentally superior to glass fiber reinforced composites?’, *Compos. Part A Appl. Sci. Manuf.*, vol. 35, no. 3, pp. 371–376, Mar. 2004.

[7] K. Oksman, Y. Aitomäki, A. P. Mathew, G. Siqueira, Q. Zhou, S. Butylina, S. Tanpichai, X. Zhou, and S. Hooshmand, ‘Review of the recent developments in cellulose nanocomposite processing’, *Compos. Part A Appl. Sci. Manuf.*, vol. 83, pp. 2–18, Apr. 2016.

[8] C. Klason, J. Kubát, and H.-E. Strömvall, ‘The Efficiency of Cellulosic Fillers in Common Thermoplastics. Part 1. Filling without Processing Aids or Coupling Agents’, *Int. J. Polym. Mater. Polym. Biomater.*, vol. 10, no. 3, pp. 159–187, Mar. 1984.

[9] R. J. Moon, A. Martini, J. Nairn, J. Simonsen, and J. Youngblood, ‘Cellulose nanomaterials review: structure, properties and nanocomposites’, *Chem. Soc. Rev. Chem. Soc. Rev*, vol. 40, no. 40, pp. 3941–3994, 2011.

[10] A. Dufresne, ‘Cellulose and Potential reinforcement’, in *Nanocellulose: From Nature to High Performance Tailored Materials*, Berlin, Boston: De Gruyter, 2017, pp. 1–42.

[11] D. Klemm, F. Kramer, S. Moritz, T. Lindstr??m, M. Ankerfors, D. Gray, and A. Dorris, ‘Nanocelluloses: A new family of nature-based materials’, *Angew. Chemie - Int. Ed.*, vol. 50, no. 24, pp. 5438–5466, 2011.

[12] A. K. Bharimalla, S. P. Deshmukh, P. G. Patil, and N. Vigneshwaran, ‘Energy Efficient Manu-facturing of Nanocellulose by Chemo-and Bio-Mechanical Processes: A Review’, *World J. Nano Sci. Engi-neering*, vol. 5, pp. 204–212, 2015.

[13] T. Saito, S. Kimura, Y. Nishiyama, and A. Isogai, ‘Cellulose Nanofibers Prepared by TEMPO-Mediated

Oxidation of Native Cellulose', *Biomacromolecules*, vol. 8, no. 8, pp. 2485–2491, Aug. 2007.

[14] H. A. Krässig, *Cellulose : structure, accessibility, and reactivity*. Gordon and Breach Science, 1993.

[15] Y. Habibi, L. A. Lucia, and O. J. Rojas, 'Cellulose nanocrystals: Chemistry, self-assembly, and applications', *Chem. Rev.*, vol. 110, no. 6, pp. 3479–3500, 2010.

[16] M. Börjesson, K. Sahlin, D. Bernin, and G. Westman, 'Increased thermal stability of nanocellulose composites by functionalization of the sulfate groups on cellulose nanocrystals with azetidinium ions', *J. Appl. Polym. Sci.*, vol. 135, no. 10, p. 45963, Mar. 2018.

[17] H. Dalväg, C. Klason, and H.-E. Strömvall, 'The Efficiency of Cellulosic Fillers in Common Thermoplastics. Part II. Filling with Processing Aids and Coupling Agents', *Int. J. Polym. Mater. Polym. Biomater.*, vol. 11, no. 1, pp. 9–38, Mar. 1985.

[18] B. V. Kokta, R. Chen, C. Daneault, and J. L. Valade, 'Use of wood fibers in thermoplastic composites', *Polym. Compos.*, vol. 4, no. 4, pp. 229–232, Oct. 1983.

[19] K. / Berggren, C. and Klason, and J. Kubat, 'Spritzgiessen holzmehlhaltiger Thermoplaste', *Kunststoffe*, vol. 65, no. 2, pp. 69–74, 1975.

[20] L. A. Berglund and T. Peijs, 'Cellulose Biocomposites—From Bulk Moldings to Nanostructured Systems', *MRS Bull.*, vol. 35, no. 3, pp. 201–207, Mar. 2010.

[21] T. Saito, S. Kimura, Y. Nishiyama, and A. Isogai, 'Cellulose Nanofibers Prepared by TEMPO-Mediated Oxidation of Native Cellulose', *Biomacromolecules*, vol. 8, no. 8, pp. 2485–2491, Aug. 2007.

[22] R. Ariño and A. Boldizar, 'Processing and mechanical properties of thermoplastic composites based on cellulose fibers and ethylene-acrylic acid copolymer', *Polym. Eng. Sci.*, vol. 52, no. 9, pp. 1951–1957, Sep. 2012.

[23] J. Zhang, S. Chen, J. Su, X. Shi, J. Jin, X. Wang, and Z. Xu, 'Non-isothermal crystallization kinetics and melting behavior of EAA with different acrylic acid content', *J. Therm. Anal. Calorim.*, vol. 97, no. 3, pp. 959–967, Sep. 2009.

[24] Y.-L. Loo, K. Wakabayashi, Y. E. Huang, R. A. Register, and B. S. Hsiao, 'Thin crystal melting produces the low-temperature endotherm in ethylene/methacrylic acid ionomers', *Polymer (Guildf).*, vol. 46, no. 14, pp. 5118–5124, Jun. 2005.

[25] R. Cooper, C. Guy, N. Seung, and K. Vredeveld, 'High Performance Copolymer Dispersions For Flexible Packaging'.

[26] M. Jonoobi, J. Harun, A. P. Mathew, and K. Oksman, 'Mechanical properties of cellulose nanofiber (CNF) reinforced polylactic acid (PLA) prepared by twin screw extrusion', *Compos. Sci. Technol.*, vol. 70, no. 12, pp. 1742–1747, Oct. 2010.

[27] a. Boldizar, C. Klason, J. Kubát, P. Näslund, and P. Sáha, 'Prehydrolyzed Cellulose as Reinforcing Filler for Thermoplastics', *Int. J. Polym. Mater.*, vol. 11, no. 4, pp. 229–262, 1987.

[28] T. H. S. Maia, N. M. Larocca, C. A. G. Beatrice, A. J. de Menezes, G. de Freitas Siqueira, L. A. Pessan, A. Dufresne, M. P. França, and A. de Almeida Lucas, 'Polyethylene cellulose nanofibrils nanocomposites', *Carbohydr. Polym.*, vol. 173, pp. 50–56, Oct. 2017.

[29] A. Junior de Menezes, G. Siqueira, A. A. S. Curvelo, and A. Dufresne, 'Extrusion and characterization of functionalized cellulose whiskers reinforced polyethylene nanocomposites', *Polymer (Guildf).*, vol. 50, no. 19, pp. 4552–4563, Sep. 2009.

[30] N. Volk, R. He, and K. Magniez, 'Enhanced homogeneity and interfacial compatibility in melt-extruded cellulose nano-fibers reinforced polyethylene via surface adsorption of poly(ethylene glycol)-block-poly(ethylene) amphiphiles', *Eur. Polym. J.*, vol. 72, pp. 270–281, 2015.

[31] H. Sehaqui, Q. Zhou, and L. A. Berglund, 'Nanostructured biocomposites of high toughness—a wood cellulose nanofiber network in ductile hydroxyethylcellulose matrix', *Soft Matter*, vol. 7, no. 16, p. 7342, 2011.

[32] Y. Srithep, L.-S. Turng, R. Sabo, and C. Clemons, 'Nanofibrillated cellulose (NFC) reinforced polyvinyl

alcohol (PVOH) nanocomposites: properties, solubility of carbon dioxide, and foaming', *Cellulose*, vol. 19, no. 4, pp. 1209–1223, Aug. 2012.

[33] V. Favier, H. Chanzy, and J. Y. Cavaille, 'Polymer Nanocomposites Reinforced by Cellulose Whiskers', *Macromolecules*, vol. 28, no. 18, pp. 6365–6367, Aug. 1995.

[34] K. Larsson, L. A. Berglund, M. Ankerfors, and T. Lindström, 'Polylactide latex/nanofibrillated cellulose bionanocomposites of high nanofibrillated cellulose content and nanopaper network structure prepared by a papermaking route', *J. Appl. Polym. Sci.*, vol. 125, no. 3, pp. 2460–2466, Aug. 2012.

[35] N. Herrera, A. P. Mathew, and K. Oksman, 'Plasticized polylactic acid/cellulose nanocomposites prepared using melt-extrusion and liquid feeding: Mechanical, thermal and optical properties', *Compos. Sci. Technol.*, vol. 106, pp. 149–155, 2015.

[36] D. Bondeson and K. Oksman, 'Polylactic acid/cellulose whisker nanocomposites modified by polyvinyl alcohol', *Compos. Part A Appl. Sci. Manuf.*, vol. 38, no. 12, pp. 2486–2492, 2007.

[37] K. Oksman, A. P. Mathew, D. Bondeson, and I. Kvien, 'Manufacturing process of cellulose whiskers/polylactic acid nanocomposites', *Compos. Sci. Technol.*, vol. 66, no. 15, pp. 2776–2784, 2006.

[38] K. Oksman, Y. Aitomäki, A. P. Mathew, G. Siqueira, Q. Zhou, S. Butylina, S. Tanpichai, X. Zhou, and S. Hooshmand, 'Review of the recent developments in cellulose nanocomposite processing', *Compos. Part A Appl. Sci. Manuf.*, vol. 83, pp. 2–18, 2016.

[39] J. Karger-Kocsis, Á. Kmetty, L. Lendvai, S. Drakopoulos, and T. Bárány, 'Water-Assisted Production of Thermoplastic Nanocomposites: A Review', *Materials (Basel).*, vol. 8, no. 1, pp. 72–95, 2014.

[40] R. Ariño and A. Boldizar, 'Processing and mechanical properties of thermoplastic composites based on cellulose fibers and ethylene-acrylic acid copolymer', *Polym. Eng. Sci.*, vol. 52, no. 9, pp. 1951–1957, Sep. 2012.

[41] I. S. Aji, S. M. Sapuan, E. S. Zainudin, and K. Abdan, 'Kenaf fibres as reinforcement for polymeric composites: A Review', 2009.

[42] D. V. Rosato, D. V. Rosato, and M. V. Rosato, *Plastic product material and process selection handbook*. Elsevier, 2004.

[43] K. L. Pickering, M. G. A. Efendy, and T. M. Le, 'A review of recent developments in natural fibre composites and their mechanical performance', *Compos. Part A Appl. Sci. Manuf.*, vol. 83, pp. 98–112, Apr. 2016.

[44] K. Sahlin, L. Forsgren, T. Moberg, D. Bernin, M. Rigdahl, and G. Westman, 'Surface treatment of cellulose nanocrystals (CNC): effects on dispersion rheology', *Cellulose*, vol. 25, no. 1, pp. 331–345, Jan. 2018.

[45] M. Hasani, E. D. Cranston, G. Westman, and D. G. Gray, 'Cationic surface functionalization of cellulose nanocrystals', *Soft Matter*, vol. 4, no. 11, pp. 2238–2244, Nov. 2008.

[46] S. Chattopadhyay, H. Keul, and M. Moeller, 'Functional Polymers Bearing Reactive Azetidinium Groups: Synthesis and Characterization', *Macromol. Chem. Phys.*, vol. 213, no. 5, pp. 500–512, Mar. 2012.

[47] T. Moberg, K. Sahlin, K. Yao, S. Geng, G. Westman, Q. Zhou, K. Oksman, and M. Rigdahl, 'Rheological properties of nanocellulose suspensions: effects of fibril/particle dimensions and surface characteristics', *Cellulose*, vol. 24, no. 6, pp. 2499–2510, Jun. 2017.

[48] E. I. and E. G. J Brandup, *Polymer Handbook, 4th Edition*, vol. 49, no. 7. Wiley-Blackwell, 1999.

[49] H. L. Cox, 'The elasticity and strength of paper and other fibrous materials', *Br. J. Appl. Phys.*, vol. 3, no. 3, pp. 72–79, Mar. 1952.

[50] J. L. Thomason and M. A. Vlug, 'Influence of fibre length and concentration on the properties of glass fibre-reinforced polypropylene: 1. Tensile and flexural modulus', *Compos. Part A Appl. Sci. Manuf.*, vol. 27, no. 6, pp. 477–484, Jan. 1996.

[51] E. Ehrnrooth and P. Kolseth, 'The Tensile Testing of Single Wood Pulp Fibers in Air and in Water', *Wood Fiber Sci.*, vol. 16, no. 4, pp. 549–566, Jun. 1984.

[52] S. Tanpichai, F. Quero, M. Nogi, H. Yano, R. J. Young, T. Lindström, W. W. Sampson, and S. J. Eichhorn, 'Effective Young's Modulus of Bacterial and Microfibrillated Cellulose Fibrils in Fibrous Networks', *Biomacromolecules*, vol. 13, no. 5, pp. 1340–1349, May 2012.

[53] F. Ansari, S. Galland, M. Johansson, C. J. G. Plummer, and L. A. Berglund, 'Cellulose nanofiber network for moisture stable, strong and ductile biocomposites and increased epoxy curing rate', *Compos. Part A Appl. Sci. Manuf.*, vol. 63, pp. 35–44, 2014.

[54] I. Diddens, B. Murphy, M. Krisch, and M. Müller, 'Anisotropic Elastic Properties of Cellulose Measured Using Inelastic X-ray Scattering', *Macromolecules*, vol. 41, no. 24, pp. 9755–9759, Dec. 2008.

[55] N. Quennouz, S. M. Hashmi, H. S. Choi, J. W. Kim, and C. O. Osuji, 'Rheology of cellulose nanofibrils in the presence of surfactants', *Soft Matter*, vol. 12, no. 1, pp. 157–164, 2016.

[56] A. Naderi, T. Lindström, and J. Sundström, 'Carboxymethylated nanofibrillated cellulose: rheological studies', *Cellulose*, vol. 21, no. 3, pp. 1561–1571, Jun. 2014.

[57] A. Naderi, T. Lindström, and J. Sundström, 'Carboxymethylated nanofibrillated cellulose: rheological studies', *Cellulose*, vol. 21, no. 3, pp. 1561–1571, Jun. 2014.

[58] T. Moberg, M. Rigdahl, M. Stading, and E. Levenstam Bragd, 'Extensional viscosity of microfibrillated cellulose suspensions', *Carbohydr. Polym.*, vol. 102, pp. 409–412, 2014.

[59] N. Wang, E. Ding, and R. Cheng, 'Thermal degradation behaviors of spherical cellulose nanocrystals with sulfate groups', *Polymer (Guildf).*, vol. 48, no. 12, pp. 3486–3493, Jun. 2007.

[60] M. A. S. Azizi Samir, F. Alloin, J.-Y. Sanchez, and A. Dufresne, 'Cellulose nanocrystals reinforced poly(oxyethylene)', *Polymer (Guildf).*, vol. 45, no. 12, pp. 4149–4157, 2004.

[61] F. Yao, Q. Wu, Y. Lei, and Y. Xu, 'Rice straw fiber-reinforced high-density polyethylene composite: Effect of fiber type and loading', *Ind. Crops Prod.*, vol. 28, no. 1, pp. 63–72, Jul. 2008.

[62] L. E. Nielsen, *Mechanical properties of polymers and composites - Vol.2*. M. Dekker, 1994.

[63] J. Kubát, M. Rigdahl, and M. Welander, 'Characterization of interfacial interactions in high density polyethylene filled with glass spheres using dynamic-mechanical analysis', *J. Appl. Polym. Sci.*, vol. 39, no. 7, pp. 1527–1539, Apr. 1990.

[64] M. Rigdahl and N. L. Salmén, 'Dynamic mechanical properties of paper: effect of density and drying restraints', *J. Mater. Sci.*, vol. 19, no. 9, pp. 2955–2961, Sep. 1984.

[65] F. Ansari, S. Galland, M. Johansson, C. J. G. Plummer, and L. A. Berglund, 'Cellulose nanofiber network for moisture stable, strong and ductile biocomposites and increased epoxy curing rate', *Compos. Part A Appl. Sci. Manuf.*, vol. 63, pp. 35–44, Aug. 2014.

[66] M. Henriksson, L. A. Berglund, P. Isaksson, T. Lindström, and T. Nishino, 'Cellulose Nanopaper Structures of High Toughness', *Biomacromolecules*, vol. 9, no. 6, pp. 1579–1585, Jun. 2008.